Bayesian inversion of a chloride profile obtained in the hydraulically undisturbed Opalinus Clay: mass transport and paleo-hydrological implications.

Catherine Yu, Julio Goncalves, Jean-Michel Matray

Elsevier Editorial System(tm) for Applied Geochemistry

Manuscript Draft

Manuscript Number:

Title: Bayesian inversion of a chloride profile obtained in the hydraulically undisturbed Opalinus Clay: mass transport and paleo-hydrological implications

Article Type: Research Paper

Keywords: Mont Terri rock laboratory, Opalinus Clay, natural tracer profile, chloride, Markov Chain Monte Carlo, leaching, diffusion

Corresponding Author: Mrs. Catherine Yu,

Corresponding Author's Institution: IRSN

First Author: Catherine Yu

Order of Authors: Catherine Yu; Julio Gonçalvès, Pr.; Jean-Michel Matray, Dr.

Abstract: The BDB-1 deep-inclined borehole was drilled at the Mont Terri rock laboratory (Switzerland) and enabled to acquire relevant data on porewater composition through the Opalinus Clay (OPA) and its bounding formations. Petrophysical measurements were carried out and included water content, water accessible porosity and grain density determination. Mobile anion profiles were obtained by aqueous leaching and out diffusion experiments performed on drillcore samples, and revealed to be consistent with previous studies carried out at the rock laboratory level. Diffusive properties were also investigated using three experimental setups: parallelepiped out diffusion, radial diffusion and through diffusion. These transport parameters were used as a priori values in a Monte Carlo Markov Chain inversion modelling approach to interpret the chloride profile in the Opalinus Clay. Based on a Peclet number analysis, a purely diffusive scenario enabled specifying the paleohydrogeological evolution of the Mont Terri site from the folding of the Jura Mountains and transport parameters.

Suggested Reviewers: Claude Degueldre Pr.
Professor of Nuclear Engineering, Engineering, Lancaster University
c.degueldre@lancaster.ac.uk

Margarita Koroleva Dr.
Geol.-Pal. Institute, Universität Hamburg
margarita.koroleva@uni-hamburg.de

Ana Maria Fernandez Dr.
Departamento de Medio Ambiente , CIEMAT
anamaria.fernandez@ciemat.es

Andreas Gautschi
Chief Geoscientific Advisor, Advisory Team Science & Technology, NAGRA
Andreas.Gautschi@nagra.ch

Paul Wersin Dr.
Institut für Geologie, University of Bern
paul.wersin@geo.unibe.ch

Title of the submitted manuscript:

Bayesian inversion of a chloride profile obtained in the hydraulically undisturbed Opalinus Clay: mass transport and paleo-hydrological implications

List of all authors' names and affiliations:

Catherine Yu[1) 2)], Julio Gonçalvès[2)], Jean-Michel Matray[1)]

1) Institut de Radioprotection et de Sûreté Nucléaire, 31 Allée du Général Leclerc, F92260 Fontenay-aux-Roses, France
2) Aix Marseille Univ., CNRS, IRD, Coll. De France, CEREGE, Aix-en-Provence, France

Short statement of the precise problem or objective addressed in the paper: (<50 words)

Understanding the salinity profile and its transient geological evolution across the Opalinus Clay at Mont Terri as a prerequisite for further transient interpretation of pressure profile.

Brief description of the essence of the approach :(<100 words)

The paper presents an exhaustive and self-consistent acquisition of transport parameters and natural tracer profiles in the hydraulically undisturbed zone crossed by the BDB-1 borehole, which is the first deep borehole drilled at the Mont Terri rock laboratory. The obtained chloride profile was interpreted by means of a purely diffusive 1D numerical model, based on a statistical approach enabling to obtain fitted parameters and associated confidence intervals.

List of the specific major novel contributions reported here :up to 3

- Consistency between data acquired at the Mont Terri tunnel level and in the hydraulically undisturbed zone crossed by the BDB-1 deep borehole.
- Confirmation of the paleohydrogeological evolution of the Mont Terri site from the folding of the Jura Mountains.

List of other journal or conference papers published or submitted that have a significant overlap with the contribution sumitted here accompanied by a brief explanation of the nature of this overlap pointing ou clearly which novel ideas submitted here have not been discussed in these prior publications:

- Acquisition of anion profiles and diffusion coefficients in the Opalinus Clay at the Mont Terri rock laboratory (Switzerland), Yu, C., Matray, J.M., 2017, Procedia Earth and Planetary Science, Vol. 17, Pages 57-60. Published

- Characterisation of anions and stable water isotopes diffusive properties in the Opalinus Clay by three experimental setups applied on BDB-1 borehole samples, C. Yu, C., Matray, J.-M., Bagagnan, S., Wittebroodt, C., Michelot, J.-L., 2017. 7th International Conference on Clays in Natural and Engineered Barriers for Radioactive Waste Confinement. Submitted and accepted for poster presentation.

These papers focused essentially on the experimental part of our work and did not detail our transport modelling at geological formation scale.

A reference to the closest prior article (by others) upon which your contributions improve:

Mazurek, M., Alt-Epping, P., Bath, A., Gimmi, T., Waber, H.N., Buschaert, S., De Cannière, P., De Craen, M., Gautschi, A., Savoye, S., Vinsot, A., Wemaere, I., Wouters, L., 2011. Natural tracer profiles across argillaceous formations. Appl. Geochem., 26, 1035-1064

Names, emails, and homepage URLs of four experts covering these areas and fields:

- Claude Degueldre, c.degueldre@lancaster.ac.uk, http://www.lancaster.ac.uk/engineering/about-us/people/claude-degueldre

- Margarita Koroleva, margarita.koroleva@uni-hamburg.de, http://4dweb.proclim.ch/4dcgi/polar/en/Detail_Person?korolevam.bern

- Jim Hendry, jim.hendry@usask.ca, http://artsandscience.usask.ca/profile/MHendry#/profile

- Martin Mazurek, martin.mazurek@geo.unibe.ch, http://4dweb.proclim.ch/4dcgi/geosciences/en/Detail_Person?mazurekm.bern

Names of the two GMOD associate editors who we believed are the most qualified to handle our paper:

Philippe Negrel and Elisa Sacchi

Technical areas and fields of expertise necessary to fully understand our contribution and to evaluate its potential and novelty:

Hydrogeology, transport modelling

Bayesian inversion of a chloride profile obtained in the hydraulically undisturbed Opalinus Clay: mass transport and paleo-hydrological implications

Catherine Yu[1) 2)], Julio Gonçalvès[2)], Jean-Michel Matray[1)]

1) Institut de Radioprotection et de Sûreté Nucléaire, 31 Allée du Général Leclerc, F92260 Fontenay-aux-Roses, France

2) Aix Marseille Univ., CNRS, IRD, Coll. De France, CEREGE, Aix-en-Provence, France

Corresponding author: Catherine Yu. E-mail: catherine.jiyu@irsn.fr

Keywords: Mont Terri rock laboratory, Opalinus Clay, natural tracer profile, chloride, Markov Chain Monte Carlo, leaching, diffusion

Abstract

The BDB-1 deep-inclined borehole was drilled at the Mont Terri rock laboratory (Switzerland) and enabled to acquire relevant data on porewater composition through the Opalinus Clay (OPA) and its bounding formations. Petrophysical measurements were carried out and included water content, water accessible porosity and grain density determination. Mobile anion profiles were obtained by aqueous leaching and out diffusion experiments performed on drillcore samples, and revealed to be consistent with previous studies carried out at the rock laboratory level. Diffusive properties were also investigated using three experimental setups: parallelepiped out diffusion, radial diffusion and through diffusion. These transport parameters were used as *a priori* values in a Monte Carlo Markov Chain inversion modelling approach to interpret the chloride profile in the Opalinus Clay. Based on a Peclet number analysis, a purely diffusive scenario enabled specifying the paleohydrogeological evolution of the Mont Terri site from the folding of the Jura Mountains and transport parameters.

1 Introduction

The Swiss National Co-operative for the Disposal of Radioactive Waste (Nagra) selected the Opalinus Clay (OPA) as a potential host rock suitable for deep geological repository of high-level radioactive waste and long-lived-intermediate-level waste. The evaluation of the confinement properties of this formation has been ongoing since 1996 in the Mont Terri rock laboratory, which is located in the Jura Mountains in north-western Switzerland. An overview of the safety aspects covered by this international research program and its contribution to the understanding of argillaceous formation behaviour was given by Bossart et al. (2017).

Solute transport is considered to be dominated by diffusion in compacted claystones due to their low permeability (Patriarche et al., 2004b; Sellin and Leupin, 2014). Limited water flow in these formations make standard sampling of porewater non applicable. Unconventional extraction processes based on physical or chemical extraction were developed and include centrifugation, squeezing, leaching, advective displacement and diffusive equilibration (Sachi et al., 2001). Natural tracer profiles across argillaceous formations give information on fluid flow and transport properties, as they result from a long-term exchange between the aquitard and the bounding aquifers porewaters (Mazurek et al., 2011; Bensenouci et al., 2013). The example of the Opalinus Clay was studied through the interpretation of several natural tracers (Cl^-, δ^2H and He) profiles by Mazurek et al. (2011). This study concluded that a purely diffusive transport model could explain the present profiles and proposed values for activation times of the Opalinus Clay bounding aquifers and initial chlorinity. However, the mainly diffusive mass transport behavior was tested by means of a sensitivity test on advection using plausible but not based on global driving forces (pressure, temperature, salinity gradients) Darcy's velocity values and no corresponding Peclet number calculation were made. In addition, only a single value of the diffusion coefficient was applied to the stratigraphic column and no uncertainties were associated with the fitting parameters.

At the end of 2014 and in the framework of the Deep Borehole experiment (DB), a 247.5 m long 45° downward inclined borehole named BDB-1 was drilled through the Opalinus Clay and the bounding formations. The aim of the experiment is to develop and validate a methodology for assessing the confinement properties of a thick argillaceous unit using the Opalinus Clay as an example. In this framework, mobile anion profiles were acquired by leaching and out diffusion experiments and diffusive transport parameters (effective diffusion coefficients and accessible porosities) were also identified by radial and through diffusion experimental setups.

This paper presents an exhaustive and self-consistent acquisition of transport parameters and natural tracer profiles in the hydraulically undisturbed zone crossed by the BDB-1 borehole. The chloride profile was interpreted by means of a purely diffusive 1D numerical model. The assumption of purely diffusive mass transport phenomena was verified by estimating the Peclet number including osmotic processes in the advection term. A bayesian inversion based on effective diffusion coefficients, initial value of the chloride concentration and two exhumation and thus hydraulic activation times for the two bounding aquifers (10 parameters) allowed to evaluate the best fit parameter sets and their uncertainties not evaluated so far. Obtaining a relevant interpretation of the chloride profile is crucial for water flow and flow characterisation. Hence, overpressures (pore pressure exceeding the hydrostatic or surrounding aquifer ones) were recognised in the Opalinus Clay and assumed so far to be remnant from its burial history (Mazurek et al., 2002). The influence of osmotic phenomena (water flow due to salinity or temperature gradients) on this pressure anomaly has not been investigated yet and depends strongly on the porewater composition. Therefore, understanding the salinity profile and its transient geological evolution across the formation is a necessary prerequisite for further transient interpretation of pressure profile (Gonçalvès et al., 2004).

2 Geological setting

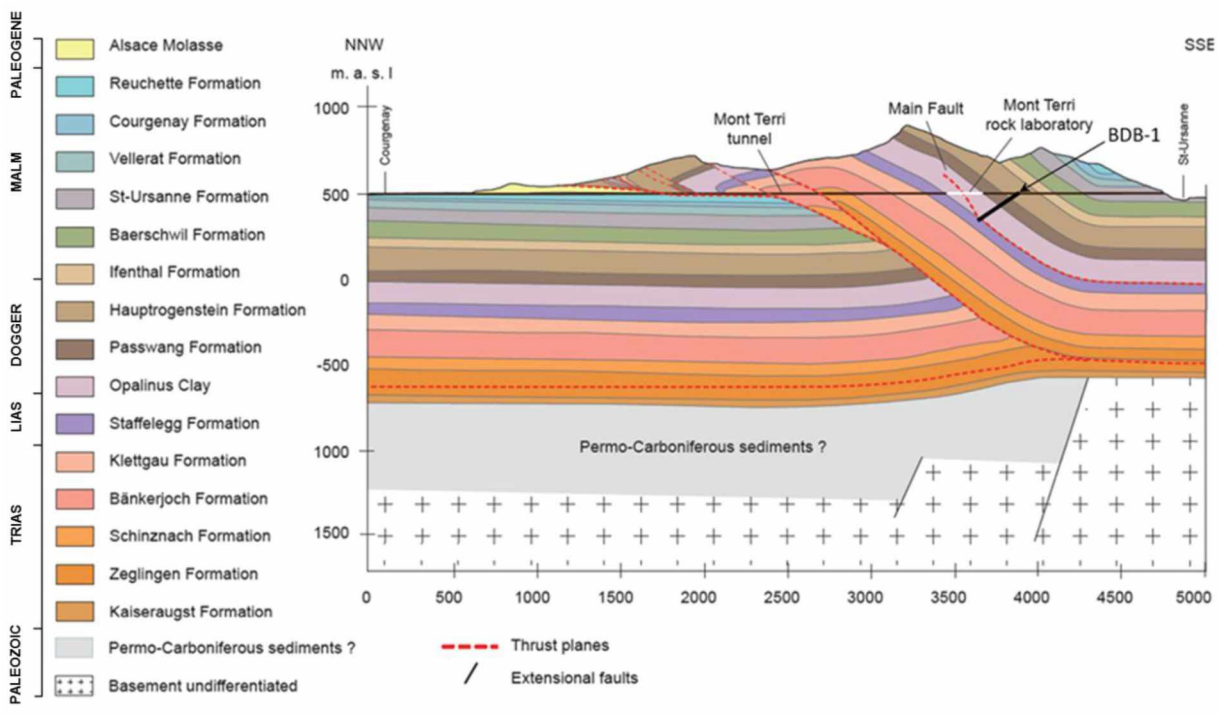

Figure 1: Geological cross-section of the Mont Terri anticline. Location of the rock laboratory is indicated by a white line. The BDB-1 deep borehole, represented by a thick black line, crosses the lower part of the Dogger aquifer, the entire Opalinus Clay formation and the upper part of the Liassic marls (adapted from Nussbaum et al., 2017).

The Opalinus Clay at the Mont Terri site is an overconsolidated claystone of Aalenian-Toarcian age, overlain by 800 m of Middle to Late Jurassic limestones, marls and shales, and underlain by 400 m of Early Jurassic to Triassic marls and limestones, dolomites and anhydrites (Figure 1). The thickness of the Opalinus Clay in the Mont Terri anticline varies between 130 m in the BDB-1 borehole and 160 m at rock laboratory level, depending on the tectonic contribution. This corresponds to a sedimentary thickness of about 120 m, when corrected for tectonic overthrusting. The Opalinus Clay reached a burial depth of 1350 m about 120 Ma ago during early Cretaceous, which resulted in a maximum temperature of 80-90°C (Mazurek et al. 2006).

A period of marine regression occurred between 100 and 40 Ma, leading to a subaerial exposure of the top of the Malm limestone. Starting about 40 Ma, the rifting of the Rhine Graben affected Northern Switzerland, resulting in considerable subsidence of the area in the mid-Tertiary, which brought the Opalinus Clay sequence back to about 500 m depth. According to Clauer et al. (2017), two sea invasions into the Mont Terri area took place during Priabonian (37 to 34 Ma) and during the Rupelian (34 to 28 Ma). Mazurek et al. (2017) proposed that the Malm limestones, represented by the Baershwil Formation, acted as a fresh-water boundary that induced a decrease of the Opalinus Clay porewater salinity to half the original value at the end of the Paleogene (23 Ma). Partial evaporation potentially occurred in the Chattian/Aquitanian and afterwards, brines would have diffused in the underlying formation, resulting in a salinity increase in the Opalinus Clay before Late Alpine folding during the late Miocene to Pliocene (about 12 to 3 Ma) that formed the Folded Jura. Erosion exposed the core of the Mont Terri anticline between 6 and 2.5 Ma, and activated the Middle Jurassic limestones aquifer (overlying the Opalinus Clay), causing a porewater flushing. Similarly, infiltration to the Early Jurassic limestones would have started in the Quaternary, between 0.5 and 0.2 Ma ago (Pearson et al., 2003, Mazurek et al., 2011).

Three main facies were identified within the Opalinus Clay (Blaesi et al., 1991): a shaly facies in the lower part of the sequence, a thin carbonate-rich sandy facies in the middle part of the formation, and a sandy facies interstratified with shaly facies in the upper sequence. The shaly facies mineral composition includes 27-78% of clay minerals (illite, chlorite, kaolinite and illite-smectite mixed layers), 4-29% of carbonates, 10-32% of quartz, and accessory feldspars, pyrite and organic matter (Bossart and Thury, 2008).

Several minor tectonic faults and a larger fault zone called “Main Fault” can be observed in the Opalinus Clay (Nussbaum et al., 2011). Nagra’s investigations in deep boreholes at Riniken, Weiach, Schafisheim and Benken revealed that the tectonically disturbed zones are

hydraulically similar to the undeformed matrix (Johns et al. 1994; Gautschi 2001a). This conclusion was also confirmed by hydraulic investigation in the BDB-1 borehole at Mont Terri (Yu et al., 2017).

3 Material and methods

3.1 Sampling

The stratigraphic sequence crossed by the BDB-1 borehole is presented in Figure 2 and is described in detail in Hostettler et al. (2017). The Opalinus Clay section was drilled with air as drilling fluid. Drilling was immediately followed by the installation of a multipacker system (Fierz and Rösli, 2014) with pressure and temperature sensors. The borehole was entirely cored for lithostratigraphic, petrophysical, mineralogical and geochemical studies. Cores sent for analysis were sampled every 10 m along the borehole. Their preservation was ensured by nitrogen flushing and sealing after vacuum with plastic foil in aluminum coated plastic bags, in order to avoid further evaporation and contact with the atmosphere.

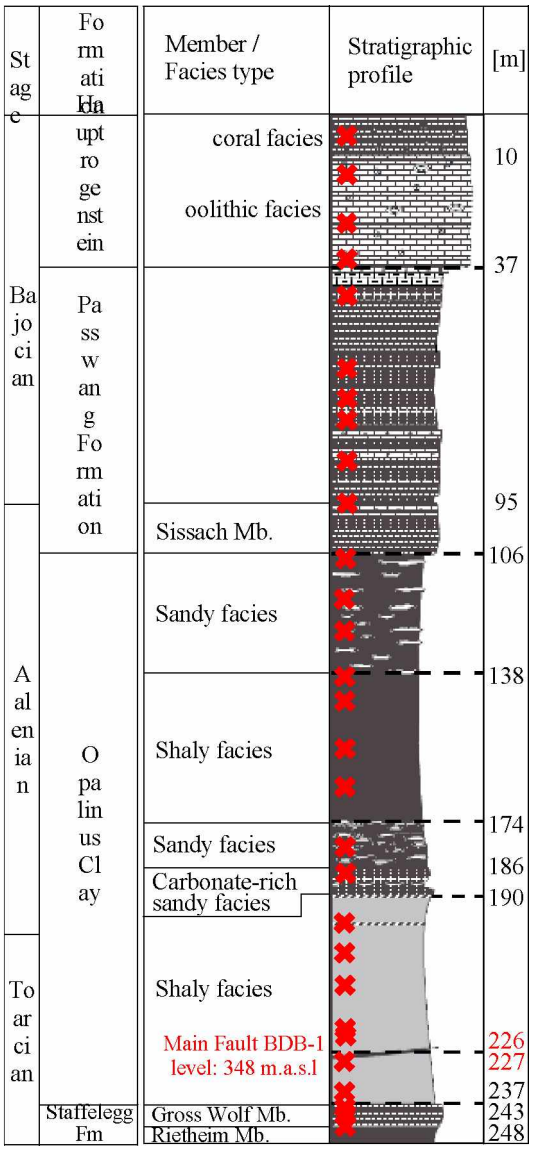

Figure 2: Lithostratigraphy of the formations crossed by BDB-1 borehole (adapted from Hostettler et al., 2017) and approximative location of the studied samples represented by red crosses.

3.2 Petrophysical characterisation

Determination of petrophysical parameters (water contents, porosity, apparent density, degree of saturation etc.) were performed in laboratory on representative elementary volume samples taken from the central part of the cores. Water contents were determined by weighing before and after oven-drying at 105 °C until mass stabilization. Density and degree of saturation were calculated based on Archimede's principle after sample immersion into kerdane (de-

aromatized hydrocarbide), following the experimental protocol first proposed by Monnier et al. (1973) and adapted to Tournemire and Mont Terri argillites (Matray et al., 2007; Matray and Möri, 2010). Grain density was evaluated using a helium pycnometer (Micromeritics Accupyc II 1340) on oven-dried samples.

3.3 Aqueous leaching

Leaching consists in diluting pore water solutes contained in a powdered rock sample into a leaching solution (Sachi et al. 2001, Koroleva et al. 2011). Samples were crushed, sieved (< 100 µm) and placed together with deionised water at solid/liquid ratio of 1:2 in centrifuge vessels. The procedure took place under controlled atmospheric condition in a glove box (N_2 atmosphere). Centrifuge tubes were placed in a hermetic glass jar and stirred out of the glove box using an end-over-end agitator during 2 hours. Then, samples were centrifuged at 10,000 rpm for 15 minutes and placed again inside the glovebox to be filtered with 0.22 µm syringe filter. Leachates were analysed by liquid ion chromatography using a Metrohm 861 Advanced Compact IC with an accuracy of 10%.

3.4 Diffusion experiments

Schematic views of the alternative experimental setups used to characterise the Opalinus Clay are shown in Figure 3.

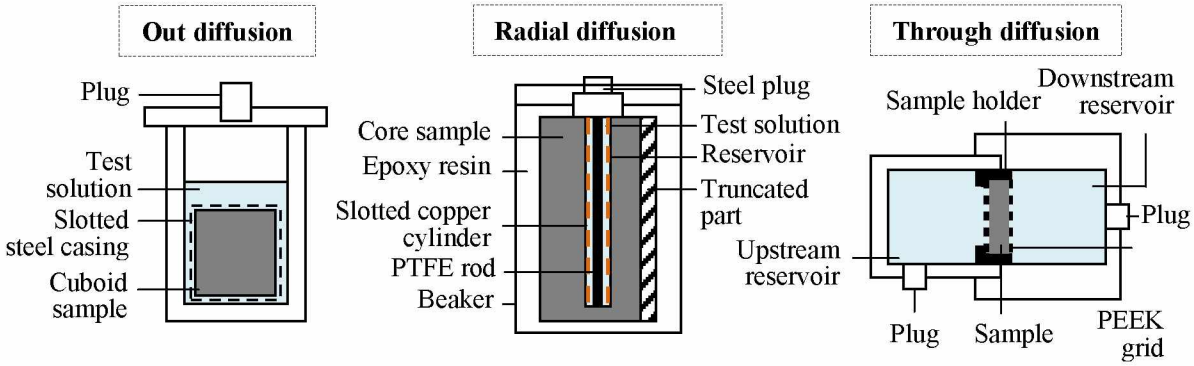

Figure 3: Schematic views of the diffusion cells used in this study to characterise the Opalinus Clay diffusive properties.

3.4.1 In and out-diffusion

In parallelepiped configuration, an out diffusion experiment consists in immersing a cubic-shaped sample into a synthetic solution and sampling the solution until reaching diffusive equilibrium. The method has been employed on argillite from Tournemire rock laboratory (France) by Patriarche (2004a) and enables the estimation of halide concentrations in porewater, as well as pore diffusion coefficient of the tested samples. Eighteen samples measuring about 5 cm wide were prepared with a diamond wire saw. They were constrained by placing a metallic grid, after being coated with epoxy resin on four faces to impose a single diffusion direction (perpendicular or parallel to the bedding). Test solutions were prepared to present a similar ionic strength to the porewater one, based on chloride contents obtained by leaching experiments.

A radial diffusion experiment consists in diffusive equilibrium between pore water contained in a drillcore and a test solution with known composition placed in an axial drilled reservoir (Van der Kamp et al. 1996, Savoye et al. 2006a and 2006b). A total of ten samples were prepared, each consisting of a core portion cut with a circular saw with a diameter of 10.2 cm or 8.5 cm and a length between 6.7 and 10 cm. A 24 mm diameter reservoir was drilled with a drill press in each sample, in which was inserted a 22 mm outer diameter copper tube with horizontal slots in order to prevent sample swelling. A 18 mm diameter polytetrafluoroethylene (PTFE) rod was also placed in the reservoir to minimise the solution volume used for the experiment and the time required to reach diffusive equilibrium. Solutions were analysed for anions (Cl^-, SO_4^{2-} and Br^-) by ionic chromatography using a DIONEX ICS-1000, and for stable isotopes (^{18}O and ^{2}H) using a Las Gatos Research LWIA-

24IEP. The analytical uncertainties of these analysis are ± 5-10 % for anions, ± 1 ‰ for ^{2}H and ± 0.6 ‰ for ^{18}O.

3.4.2 Through diffusion

Through diffusion cells consisted of a polypropylene sample holder, two polypropylene reservoirs for liquid phase (upstream and downstream, with respective capacities of 180 mL and 90 mL), two supporting grids and two sampling openings. Six cylindrical samples of approximatively 10 mm thickness and 30 mm diameter were prepared from core samples by sawing with a diamond wire saw. These samples were confined between porous polyether ether ketone (PEEK) grids in order to control clay mineral swelling and the assembly was fixed to the sample holder using Sikadur® epoxy adhesive. After a resaturation phase with synthetic porewater, the solutions were replaced with fresh ones and the upstream reservoir added with conservative radioactive tracers (HTO and $^{36}Cl^{-}$). The flux of radioactive species between the reservoirs was monitored as a function of time by liquid scintillation using a Packard Tri-carb 3100 TR counter. The accuracy of activity measurement is estimated at 6.4% for HTO and 3.5% for $^{36}Cl^{-}$.

3.4.3 Modelling of the diffusion experiments

Parallelepiped out diffusion and through diffusion experiments were modelled numerically using the chemistry-transport coupled model code HYTEC (Van der Lee et al. 2003), which is based on finite volumes method. In purely diffusive system and for mobile components, the transport equation writes:

$$\omega \frac{\partial c_i}{\partial t} = \text{div}\,(D_e \nabla c_i) \qquad (1)$$

where c_i is the total concentration of component i, ω [-] is the diffusion accessible porosity for mobile components, and D_e [m^2 s^{-1}] is the effective diffusion coefficient with $D_e = \omega D_p$, where D_p is the pore diffusion coefficient accounting for the tortuosity of the porous media.

For radial diffusion experiments, a numerical inversion of the semi-analytical solution given by Novakowski and Van der Kamp (1996) and Savoye et al. (2006b) was applied using Mathematica 5.2©.

3.5 Markov Chain Monte Carlo inversion approach

The chloride profile acquired on samples from the BDB-1 borehole was interpreted using a finite difference numerical resolution of the transport equation (1). This numerical treatment, which includes a statistical inversion process using a Markov Chain Monte Carlo (MCMC) algorithm (Metropolis), was implemented using Python©. MCMC methods are probabilistic sampling techniques for Bayesian parameter estimation and uncertainty quantification. The basic principle consists in an oriented random walk exploration of the parameter space in order to avoid large time-consuming and even unrealistic systematic (using regular steps) sampling of parameters sets that allow reproducing the chloride profile. Each selected parameters set throughout the random walk is introduced in direct transport simulations. Therefore, these algorithms generate a sequence of model parameter sets and compare the model-based predictions to a given set of observed measurements (Tarantola, 2005; Gallagher et al. 2009; Petersen et al. 2014). The model parameters are constrained to minimise the misfit between simulated (sim_i) and measured values (obs_i), represented here by the mean squared error function $S(\boldsymbol{m})$:

$$S(\boldsymbol{m}) = \frac{1}{n}\sum_{i}(obs_i - sim_i)^2 \qquad (2)$$

where n is the number of measurements and $\boldsymbol{m}(m_1 \ldots m_n)$ is the vector of model parameters.

The random walk is based on sorted values in the *a priori* probability density function (pdf) $\rho(\boldsymbol{m})$ of each parameter while the forward modelling identifies a set of parameters allowing a good agreement between simulated and observed chloride values. This set of successful

parameters samples the *a posteriori* joint pdf $\sigma(\boldsymbol{m})$ which describes the updated parameters distribution (after forward modelling and data comparison) yielding the best simulations. Then, marginal pdfs have to be identified for each parameter to estimate e.g., its mean value and associated uncertainty. A complex mathematical treatment is required to assess rigorously the marginal pdf of each parameter. Alternatively, the marginal distributions can be simply identified by a statistical treatment of all the parameters samples that satisfy an acceptance criterion (fraction of best simulations, misfit threshold). For the sake of simplicity, the marginal pdf were identified using the second alternative approach.

Let's now consider a current step of the MCMC algorithm characterised by a position $\boldsymbol{m}_i$ of the random walk in the parameter space, and a potentially new position $\boldsymbol{m}_j$ created by means of a random perturbation of $\boldsymbol{m}_i$. The acceptance of the displacement from a former parameter set $\boldsymbol{m}_i$ to the posterior one $\boldsymbol{m}_j$ follows the probabilistic rule (probability of acceptance P):

$$P\begin{cases} 1 & if\ S(\boldsymbol{m}_i) > S(\boldsymbol{m}_j) \\ \dfrac{L(\boldsymbol{m}_j)}{L(\boldsymbol{m}_i)} = \exp\left(-\dfrac{\Delta S}{\alpha}\right) & if\ S(\boldsymbol{m}_i) < S(\boldsymbol{m}_j) \end{cases} \tag{3}$$

where $L(\boldsymbol{m})$ is the likelihood function defined by :

$$L(\boldsymbol{m}) = k \times e^{-\frac{S(m)}{\alpha}} \tag{4}$$

where k is a normative constant that ensures that the integral of $\sigma(\boldsymbol{m})$ over the parameter space equals 1, α is a convergence parameter to be set here by trial and error, and $exp(-\Delta S/\alpha) = exp(-(S(\boldsymbol{m}_j)-S(\boldsymbol{m}_i))/\alpha)$.

The first option in equation (3) just states that if the displacement yields a lower error between the direct model results and the observations, the displacement is accepted. The second one states that an unfavourable displacement can be accepted in order to leave local minimum values of the objective function and to explore other regions of the parameter space. This

second option is practically treated by sorting a value in an uniform distribution between 0 and 1: if it is lower than $exp(-\Delta S/\alpha)$, which occurs with a probability $exp(-\Delta S/\alpha)$, then the unfavourable displacement is accepted and the algorithm (Eq. 3) is satisfied. This algorithm globally favours the displacements within the parameter space in the direction of decreasing misfits. After a first convergence stage of the method, which consists in reaching the regions of the parameter space where the error is minimum, the MCMC algorithm provides a set of accepted parameters which allow the best simulations.

4 Results and discussion

4.1 Transport parameters

4.1.1 Porosities

Porosity values obtained from petrophysical analysis and diffusion experiments are reported in Figure 4.

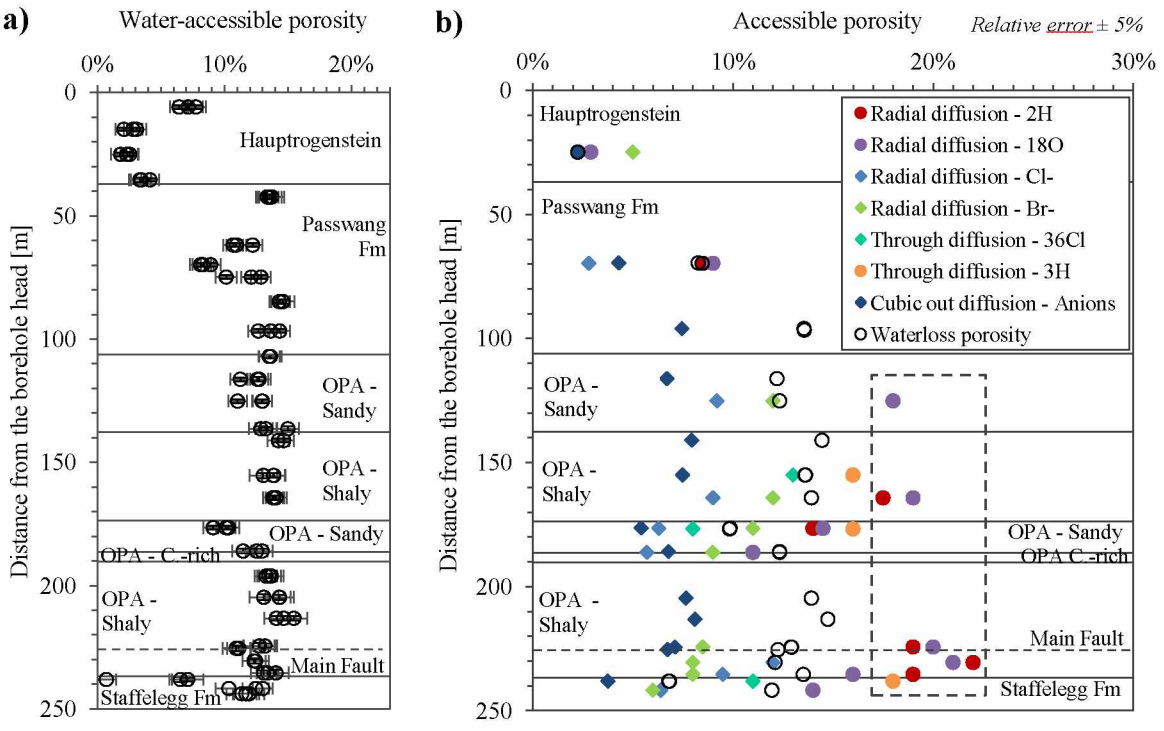

Figure 4: a) Water accessible porosity acquired by oven-drying at 105°C of BDB-1 borehole samples and b) accessible porosity to anions (Cl^-, Br^-), radioactive tracers (HTO, $^{36}Cl^-$) and

stable water isotopes (^{3}H, ^{18}O) determined by laboratory-scale diffusion experiments. Values framed by a dashed line are probably overestimated due to swelling or microcracks.

The mean water accessible porosity determined by density measurements is 13.0% in the Opalinus Clay, with a lower average porosity of 12.0% in the sandy facies compared to the shaly facies, which shows a mean porosity of 13.5%. These values are lower than the mean value of 18% suggested by previous studies performed at the Mont Terri tunnel level (Bossart et al. 2017). The Passwang Formation presents slightly lower porosity values ranging between 8.1% and 14.6% with a mean value of 12.2%. The Hauptrogenstein is characterised by the lowest porosity with a mean value of 3.9%.

Except for the carbonate-rich sandy facies, porosity values obtained by radial diffusion for stable water isotopes in the Opalinus Clay (up to 22 %) are higher than the values obtained by density measurements (maximum value of 15 %). Sample preparation steps, such as drilling, may have brought additional porosity by creating microcracks. Values obtained for ^{2}H and ^{18}O are globally comparable and the anion exclusion (ratio of anion to water accessible porosities) is in the range of 51 % to 55 % in the OPA shaly facies and between 45 % and 51 % in the sandy facies. These results are consistent with the ratio of 55%, which was chosen in out diffusion experiments to calculate anion contents in porewater and based on literature data (Pearson et al. 2003). Chloride and bromide diffusion accessible porosities are also comparable with values ranging between 6 % and 12 % and a best estimate at 8%.

4.1.2 Diffusion coefficients

Deduced from radial diffusion experiments, chloride and bromide effective diffusion coefficient parallel to the bedding are in the order of 4.0×10^{-11} m^2 s^{-1} in the Opalinus Clay, which is in good agreement with the range of 1.7×10^{-11} to 4.5×10^{-11} m^2 s^{-1} for bromide and 1.8×10^{-11} to 6.8×10^{-11} m^2 s^{-1} for chloride reported in previous studies (Bossart et al. 2011). Reasonable values from 3.0×10^{-11} to 1.1×10^{-10} m^2 s^{-1} are obtained for stable water isotopes.

Values obtained by through diffusion experiments are also in good agreement with literature data. In the Opalinus Clay shaly facies, values of 9.6×10^{-11} m^2 s^{-1} for tritium and 1.4×10^{-11} m^2 s^{-1} for ^{36}Cl are obtained parallel to the bedding. In the sandy facies, simulations give 1.9×10^{-11} m^2 s^{-1} for tritium and 5.1×10^{-12} m^2 s^{-1} for ^{36}Cl perpendicular to the bedding (Figure 5). Due to experimental artefacts linked to sample preparation, only three out of the six through diffusion cells provided relevant data.

Alternative formula for the anion exclusion ratio is given by Jacquier et al. (2013) and writes:

$$P_a = \frac{D_e[HTO]/D_e[^{36}Cl^-]}{D_0[HTO]/D_0[^{36}Cl^-]} \quad (5)$$

where D_e [m^2 s^{-1}] is the effective diffusion coefficient and D_0 [m^2 s^{-1}] is the diffusion coefficient in free water, equal to 2.008×10^{-9} m^2 s^{-1} for HTO and 1.771×10^{-9} m^2 s^{-1} for Cl^- at 25°C (Mills and Lobo, 1989).

Using equation (5), the diffusion anion exclusion deduced from through diffusion experiment is equal to 5.9 in the Opalinus Clay shaly facies, and 3.2 in the sandy facies.

The diffusion anisotropy ratio is the ratio between the effective diffusion coefficients parallel and perpendicular to the bedding. Based on out diffusion experiments, a low anisotropy ratio of 2.4 was estimated for chloride effective diffusion coefficient in the Opalinus Clay sandy facies, which is lower than the value of 4 reported by Van Loon et al. (2004) on a shaly facies sample. Anisotropy of diffusive parameters could not be determined in the shaly facies due to sample cracking and other unloading artefacts.

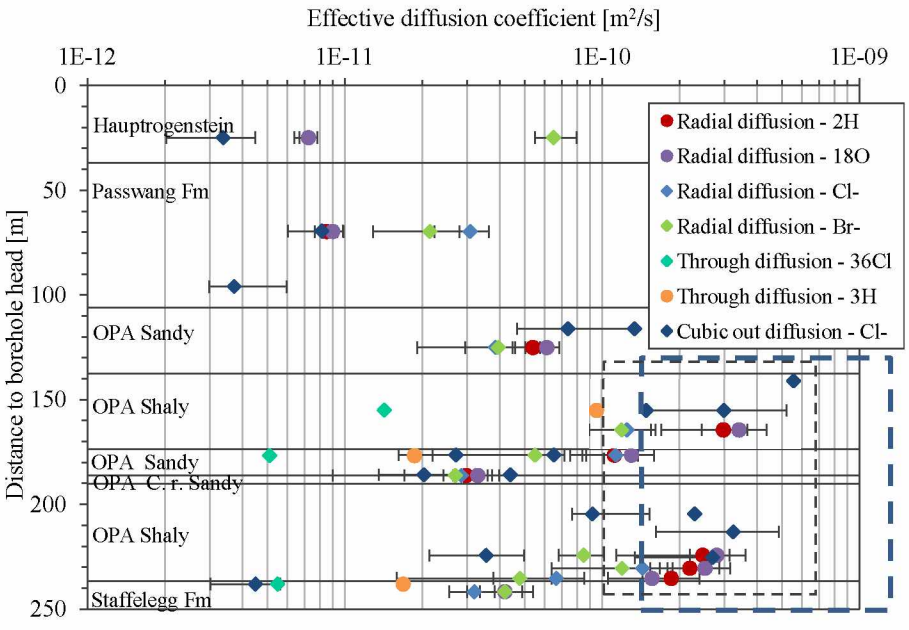

Figure 5: Effective diffusion coefficients acquired on BDB-1 borehole samples. Values framed by a dashed line are probably overestimated due to swelling or microcracks.

4.2 Anion profiles

Chloride, bromide and sulphate profiles acquired by leaching and out diffusion experiments on BDB-1 samples are presented in Figure 6 and confirm the vertical variability of porewater composition along the stratigraphic column.

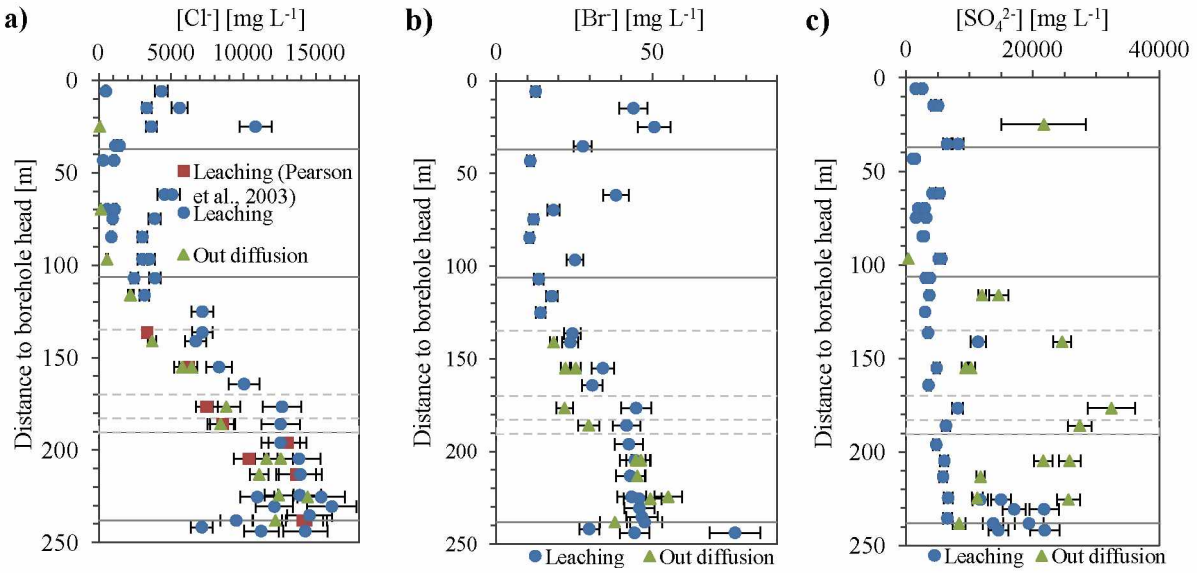

Figure 6: Chloride, bromide and sulphate profiles acquired along BDB-1 borehole by leaching experiments and out diffusion tests.

Chloride and bromide values obtained by aqueous leaching are systematically higher compared to out diffusion results. Higher values of halides given by aqueous leaching compared to out diffusion are likely due to mineral dissolution or release of elements initially contained in inaccessible porosity. However, the two methods reveal similar curved profiles with increasing chlorinity towards the basal part of the Opalinus Clay (up to 16.1 g L^{-1} from leaching experiments). Out diffusion experiments give a range between 2.1 ± 0.3 g L^{-1} and 14.4 ± 1.0 g L^{-1} for chloride contents with maximum concentrations found in the basal shaly facies of the Opalinus Clay. The sulphate profile along BDB-1 borehole also shows an increasing trend with depth, but even when extraction was performed under anoxic conditions, oxidation had a major effect on measured concentrations. Artificial increase of sulphate contents can be induced by artefacts linked to experimental procedures: pyrite oxidation during the sample preparation or equilibration process, and dissolution of sulphate-bearing minerals such as gypsum or celestite (Pearson et al., 2003; Wersin et al., 2013). Previous studies conducted at the tunnel level also concluded to a maximum value ranging from 13.6 to 14.4 g L^{-1} for chloride content, found at the limit between the Opalinus Clay and the Staffelegg Formation (Pearson et al. 2003). The halide concentration ratios are consistent with a marine origin of the Opalinus Clay porewater.

4.3 Chloride profile modelling

4.3.1 Modelling assumptions and scenario

Although the predominant character of diffusion among other transport processes in low permeability formations is generally claimed, such assumption, which greatly simplifies transport numerical calculations, must be verified using the Peclet number (Soler, 2001):

$$Pe = \frac{qL}{D_e} \quad (6)$$

where q [m s^{-1}] is the specific discharge (Darcy's velocity), L [m] is a characteristic distance for transport, here taken to be the formation half thickness, and De [m^2 s^{-1}] is the effective diffusion coefficient. It is classically stated that for Pe < 1, diffusion dominates over advection and advection is dominant over chemical diffusion if Pe > 1. However, in their discussion of transport phenomena in low permeability environments, Huysmans and Dassargues (2005) show that for Peclet numbers (Eq. 6) as high as 10, numerically simulated salinity profiles considering advection and diffusion or diffusion alone only differed by 10% pointing to a negligible advective contribution. Consequently, one can consider that below a value of 10 for Pe, diffusion models are sufficiently accurate for salinity profile interpretations.

The Opalinus Clay formation is characterized by maximum pressures (or hydraulic head h) and chlorinity values within the formation yielding corresponding differences with the surrounding aquifers of at least 5 bars (Δh = 50 m) and Δc = 0.42 mol L^{-1} respectively. A monotonic cross-formational temperature difference of 8°C per 100 m is also observed.

Considering that osmotic processes are at work in the Opalinus Clay, the 1D Darcy's velocity accounting for osmotic terms can be expressed as (Gonçalvès et al., 2015):

$$q = -K\frac{\partial h}{\partial z} + \frac{\nu RT\varepsilon_c K}{\rho g}\frac{\partial c}{\partial z} - \frac{\varepsilon_T}{\rho g}K\frac{\partial T}{\partial z} \quad (7)$$

where K [m s^{-1}] is the cross-formational hydraulic conductivity, z is the axis perpendicular to the bedding, h [m] is the hydraulic head, ρ is the porewater density [kg m^{-3}], g [9.81 m s^{-2}] is the gravitational acceleration, ε_c[-] and ε_T [Pa K^{-1}] are respectively the chemical osmotic efficiency and the thermo-osmotic coefficient, ν is the number of dissociated species for a salt (e.g. 2 for NaCl), R [8.32 m^3 Pa K^{-1} mol^{-1}] is the gas constant, T [K] is the temperature, and c

[mol m^{-3}] is the chloride concentration. Note that for this first-order calculation, no gravity effect due to salinity is considered enabling the use of the hydraulic head h.

The first term in the right-hand side of Equation (7) is related to purely darcian fluid flow, the second and third terms to the chemical and thermal osmosis, i.e. fluid flow driven by salinity and temperature gradients. The petrophysical parameters of the Opalinus clay together with the thermo-osmotic model by Gonçalvès et al. (2015) points to a negligible thermo-osmotic term here. For the two remaining terms, simple gradients given by $\Delta h/L$ and $\Delta c/L$ can be introduced in Eqs (6) and (7). Peclet calculations require equivalent transport parameters (harmonic means across the formation, perpendicular to the bedding). Using the data of this study and of Yu et al. (2017), a harmonic mean of 10^{-11} m^2 s^{-1} and 1.85×10^{-13} m s^{-1} is found for D_e and K. Using these values for an equivalent NaCl ($v = 2$) system and ε_c between 0.036 and 0.081 (Noy et al., 2004) yields a Peclet number of between 0.6 and 0.8. It can thus be concluded that transport is likely dominated by diffusion for the Opalinus Clay. Therefore, mass transport calculations can be made by solving Equation (1) using a simple and robust finite difference numerical scheme.

The paleohydrogeological evolution was chosen accordingly to the conclusions of Bossart and Wermeille (2003), who constrained the erosion and thus the exhumation of the Dogger limestone overlying the Opalinus Clay between 10.5 and 1.2 Ma (time t_0 hereafter). At that time, the subsequent rapid flushing of the Dogger limestone pore water by meteoritic water brought the salinity to zero which constitutes a boundary condition for the transport model. The activation of the Liassic limestone aquifer underlying the Opalinus Clay occurred between 0.5 and 0.2 Ma (time t_1). A plausible range between 14 and 23 g L^{-1} was chosen for the initial chlorinity C_0 prior to the Jura Mountains folding (Mazurek et al., 2011). Cross-formational diffusive transport parameters, namely effective diffusion coefficient and diffusion accessible porosity, were deduced from laboratory experiments carried out on BDB-

1 samples and described in section 5.1. Exhumation times t_0 and t_1 together with the initial chlorinity are used for boundary and initial conditions definition of the 1D diffusion model. At initial time t_0, the chlorinity is set to C_0 within the Opalinus clay, the upper and lower concentration boundary conditions are 0 and C_0, respectively. Then, when the simulation time reaches t_1, the lower boundary condition is set to zero. These boundary conditions allow simulating diverging diffusive mass transport from the Opalinus Clay towards first the upper aquifer alone then towards both aquifers. The model takes into accounts 7 formations showing different properties listed in Table 1.

4.3.2 Modelling results

The parameters to be calibrated must be chosen carefully since for more than 10 parameters, implementing MCMC methods becomes hazardous (large time- and cpu-consuming, convergence issues). However, under the assumption of purely diffusive mass transport, since the porosity intrinsically appears ($D_e = \omega D_p$) in both sides of Equation (1), this parameter does not impact calculated chlorinity profiles which are only controlled by the pore diffusion coefficient. Therefore, porosity was not considered in our inverse modelling and was kept constant for each formation. From a practical standpoint, the calibrated parameters were the cross-formational effective diffusion coefficient for each of the 7 formations D_e (in fact D_p since ω is fixed, see above), t_0, t_1 and C_0 which are all considered uncertain. Uniform *a priori* distributions were considered for these 10 parameters using lower and upper boundaries described in Section 4.3.1 for t_0, t_1 and C_0, and boundaries encompassing the measurements for the 7 formation D_e values (see Table 1)

In the course of the MCMC inversion process involving 10 parameters (a priori values in Table 1), the misfit function reached a plateau after about 2000 iterations for 100000 performed iterations (Figure A.1, Appendix A). Only about 800 random moves were accepted,

indicating a relatively low number of parameter sets that fit the experimental data. The sets of parameters leading to the 5% lower misfit values were used to establish the *a posteriori* marginal distributions of the ten parameters shown in Fig 2.A of Appendix A. Both multimodal and unimodal distributions are obtained. Multimodal distributions were fitted by gaussian mixture distributions, all unimodal variables were fitted by a gaussian model except for C_0 that is described by a log normal distribution (see Appendix A). Mean values and 95% confidence intervals for each parameters were calculated using the fitted distributions (see Table 1). For multimodal distributions, the weights and means of each fitted normal distribution component are used to calculate an "overall mean" for a given parameter as the weighted average of the mean values (see Appendix A). Therefore, the relative importance of each gaussian distribution within the gaussian mixture is respected. Note that the low number of sampled values in the parameter space is likely a limitation for the *a posteriori* marginal pdfs identification method described in Section 3.5. However, taking more samples (40% of accepted displacements) yields the same type of marginal distributions but with slightly different statistical parameters and a larger misfit when the mean parameters values are used in a direct simulation.

Table 1: Input parameters and associated uncertainties involved in the MCMC inversion process. Accessible porosities and formation thicknesses were kept constant. CI stands for Confidence Interval.

Formation	Thickness [m]	ω [vol.%]	De [m^2/s] ($\times 10^{-11}$) *Measurements*	*A priori*	*A posteriori Mean and 95% CI*
Passwang Formation	69	7.5	D_e^7: 0.817 ± 0.2	[10^{-1}-20]	2.66 [1.51; 4.81]
OPA – Sandy facies	29	6.9	D_e^6: 7.38 ± 4.36	[10^{-1}-20]	6.55 [3.92; 11.61]
OPA – Shaly facies	35	7.6	D_e^5: 0.597 ± 0.2	[10^{-1}-20]	0.30 [0.18; 0.41]
OPA –	14	5.4	D_e^4: 2.71	[10^{-1}-20]	1.91

Sandy facies			± 1.9		[0.59; 4.12]
OPA – Carbonate-rich Sandy facies	6	6.8	D_e^3: 2.04 ± 0.68	[10^{-1}-20]	2.91 [0.39; 4.84]
OPA – Shaly facies	47	7.7	D_e^2: 3.56 ± 1.42	[10^{-1}-20]	0.33 [0.04; 0.62]
Staffelegg Formation	63	4.5	D_e^1: 0.451 ± 0.132	[10^{-1}-20]	0.59 [0.15; 1.04]

Parameter	Value	Range			
	A priori				*A posteriori*
Activation time [Ma]					
Dogger aquifer (upper boundary)	-5	[-10.5; -1.2]			-4.54 [-6.77; 1.7]
Lias aquifer (lower boundary)	-0.25	[-0.5;-0.2]			-0.24 [-0.3; -0.2]
Initial chlorinity [g L^{-1}]	19	[14;23]			19 [17.3; 22]

As shown in Figure 7a, the simulation of diffusion for chloride matches fairly well the experimental data considering the mean a posteriori values for the parameters (Table 1). Except for two diffusion coefficients values (Passwang Formation and Opalinus Clay basal shaly facies), the fitted parameters are highly consistent with the measurements and exhumation time expectations (Figure 7b). The misfit for diffusion coefficients can be due to an imperfect mechanical confining of the Opalinus Clay sample leading to an overestimation of the measured D_e for the Opalinus Clay shaly facies. On the other hand, the Passwang Formation is more heterogeneous compared to the different facies of the Opalinus Clay. Lithostratigraphic investigation carried out by Hostettler et al. (2017) on BDB-1 drillcores showed that this formation exhibits variable lithology (silty to fine sandy marls, quartz sand and biodetrital sandy limestones, ferruginous limestones, iron oolithic marls and limestones). The number of samples investigated in laboratory-scale diffusion experiments was likely insufficient to reflect this variability in the present study.

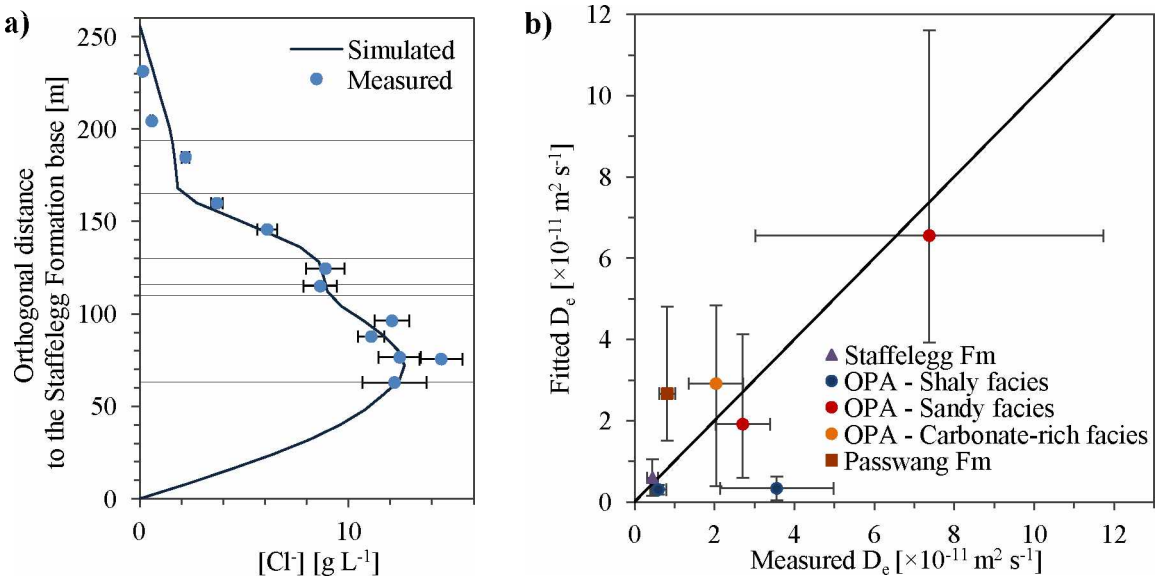

Figure 7: Comparison between a) experimental and simulated chloride profile obtained with the mean *a posteriori* values for the parameters and b) experimental and fitted diffusion coefficients, error bars represent 95% confidence interval.

The modelling results are globally consistent with previous studies carried out at the Mont Terri rock laboratory. A lower equivalent effective diffusion coefficient for anions of 4.6×10^{-12} m² s^{-1} was used in Mazurek et al. (2011) for the Opalinus Clay and the directly adjacent formations, whereas different diffusion coefficient values were considered for each unit along the rock sequence in the present study. A higher cross-formational equivalent diffusion coefficient of 6.3×10^{-12} m² s^{-1} for the Opalinus Clay explains the shorter time obtained for the adjacent aquifers activation in comparison with the study of Mazurek et al.(2011): 4.5 Ma compared to 6 Ma for the upper aquifer and 0.246 Ma compared to 0.5 Ma for the lower aquifer. However, the activation age at -4.54 Ma proposed here is close to one of the major morpho-tectonic event proposed by Kuhlemann and Rahn (2013) at -4.2 Ma.

5 Conclusions

An integrated study from BDB-1 borehole samples characterisation on the Opalinus Clay transport capabilities and transport modelling was performed. Petrophysical analysis enabled

the acquisition of water accessible porosity, grain density and water contents along the rock sequence. Out diffusion and aqueous leaching techniques were used to obtain chloride concentrations of porewater in the Opalinus Clay and its bounding formations. Effective diffusion coefficients and diffusion accessible porosities were also investigated by radial diffusion and through diffusion experiments.

The measured chloride contents are in good agreement with previous investigation performed at the Mont Terri tunnel level, and show an asymmetric bell-shaped trend increasing to a high chloride concentration of 14.4 g L^{-1} towards the bottom of the Opalinus Clay. Moreover, chloride to bromide ratios reflect a marine signature in the clay rock. The chloride profile suggests a diffusive exchange between the argillaceous formation and the adjacent aquifers, with deferred activation times of the fresh-water sources linked to the surface erosion of the geological formations. This scenario was implemented in a Monte Carlo Markov Chain algorithm, which enabled to assess the best fitting set of parameters (initial chloride content, aquifer activation times and diffusion coefficients) and associated confidence intervals explaining the present-day chloride profile. Experimental and simulated data are comparable for respective diffusion times of 4.54 Ma and 0.246 Ma between the Opalinus Clay and the Dogger (overlying) and Liassic (underlying) limestones.

The present study confirms the paleohydrogeological evolution of the Mont Terri site from the folding of the Jura Mountains. This scenario is fundamental to constrain our future transient modelling of the overpressure regime observed in the Opalinus Clay to fully characterise transport processes in this formation.

Acknowledgments

This study was performed in the framework of the Deep Borehole experiment, financed by six partners of the International Mont Terri Consortium (Swisstopo, NAGRA, BGR, GRS, NWMO, IRSN).

Appendix A

The convergence of the MCMC approach is characterised by a sharp decrease of the misfit function value from almost 7 to 1.5 on average after 2000 iterations (almost 200 accepted movements) of the random walk as shown in Figure A.1.

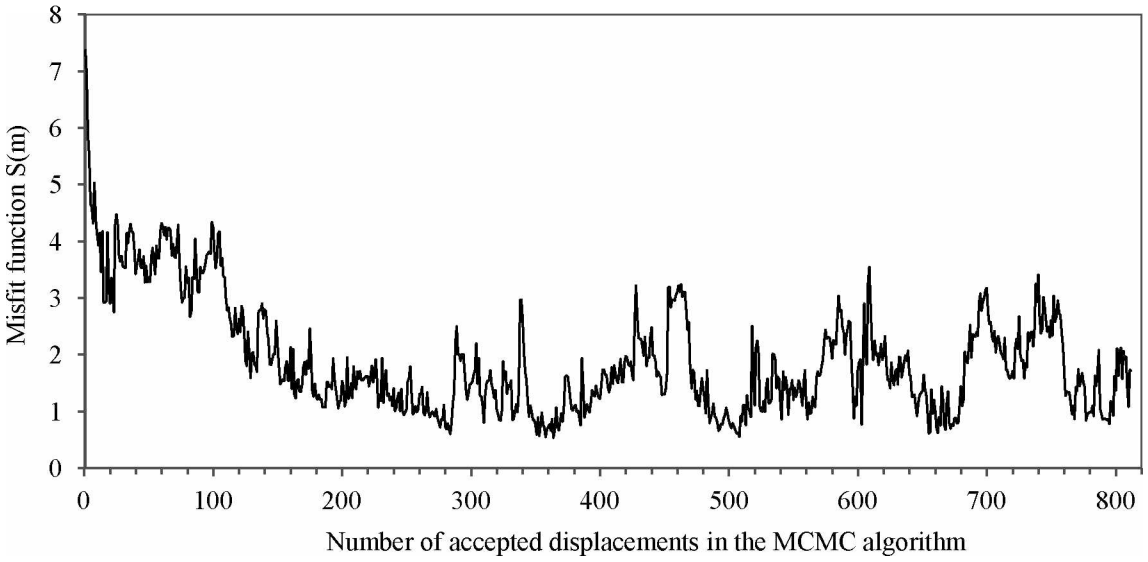

Figure A.1: Misfit function as a function of the number of accepted displacements in the MCMC algorithm.

The sets of parameters leading to the 5% lower misfit values (errors lower than 0.7) were used to establish the *a posteriori* marginal distributions (Figure A.2).

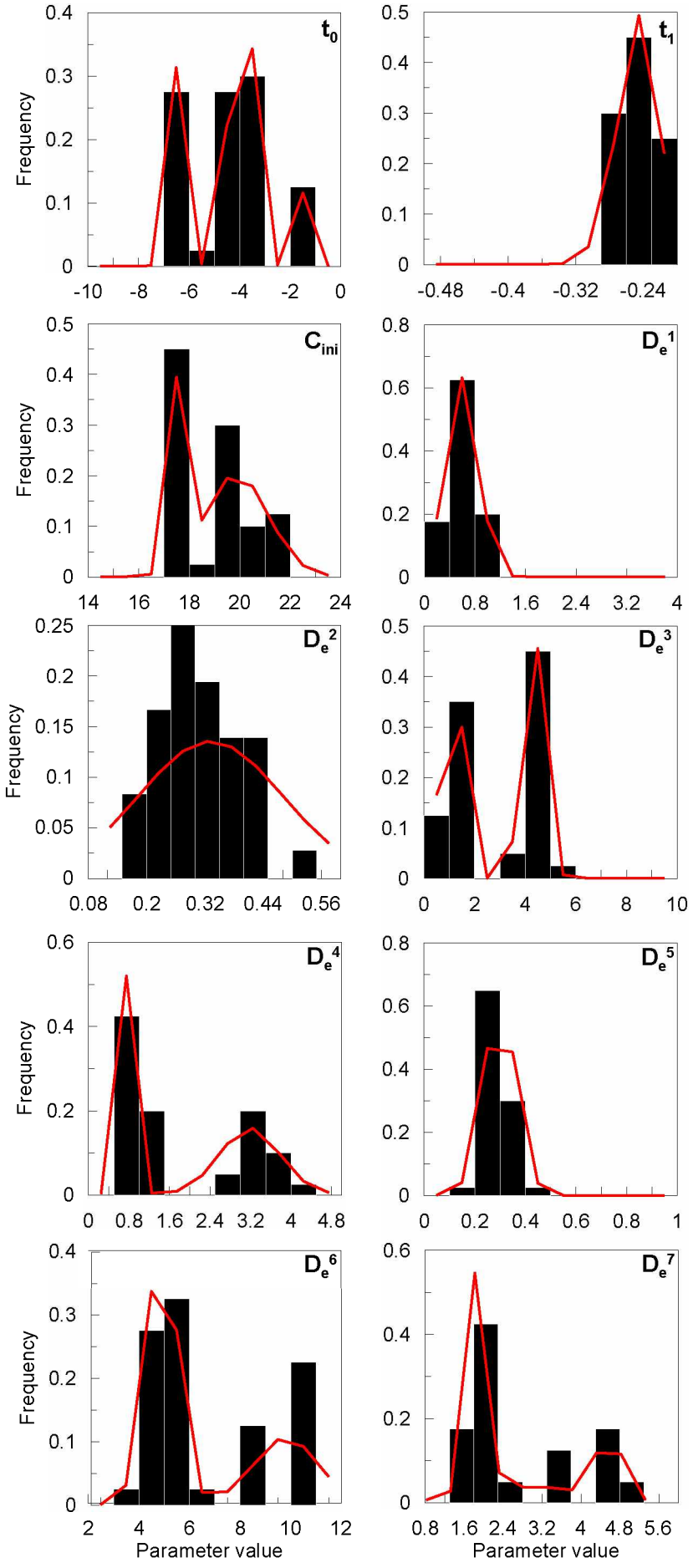
t0
t1
Cini
De1
De2
De3
De4
De5
De6
De7
Frequency
Parameter value

489

Figure A.2: *A posteriori* distributions (pdfs) for each parameter of the diffusion model. Parameters values in [$\times 10^{-11}$ m^2 s^{-1}] for De, [g L^{-1}] for C_0, and [Ma] for t_0 and t_1. The histograms results from the MCMC approach (Section 3.5). In red, the fitted theoretical distributions (Gaussian mixtures: t_0, C_0, D_e^3, D_e^4, D_e^6, and D_e^7, Gaussian: D_e^1, D_e^2, and D_e^5, and Lognormal: t_1)

Multimodal distributions were fitted by gaussian mixture distributions:

$$\alpha G(\mu_1, \sigma_1) + \beta G(\mu_2, \sigma_2) + \gamma G(\mu_3, \sigma_3) \quad \text{(A.1)}$$

where $G(\mu_i, \sigma_i)_{i=\{1,..3\}}$ are Gaussian distributions and α, β, and γ are the respective weights. The fitted distribution parameters are listed in Table A.1.

Table A.1: Parameters of fitted pdf with effective diffusion coefficients D_e [$\times$ 10^{-11} m^2 s^{-1}], activation times t_0 and t_1 [Ma], and initial chloride concentration C_0 [g L^{-1}].

Variable	α	β	γ	μ_1	σ_1	μ_2	σ_2	μ_3	σ_3
t_0	0.32	0.56	0.12	-6.45	-3.95	-1.78	0.19	0.22	0.10
Log(-t_1)	1	0	0	-0.61	0.04	-	-	-	-
C_0	0.37	0.63	0	17.48	19.87	1.22	0.09	-	-
D_e^1	1	0	0	0.60	0.22	-	-	-	-
D_e^2	1	0	0	0.33	0.14	-	-	-	-
D_e^3	0.16	0.3	0.54	0.48	1.74	4.33	0.08	0.08	0.3
D_e^4	0.53	0.47	0	0.75	3.18	0.57	0.10	-	-
D_e^5	1	0	0	0.3	0.06	-	-	-	-
D_e^6	0.67	0.33	0	4.91	9.83	1.24	0.55	-	-
D_e^7	0.58	0.22	0.2	1.86	3.08	4.58	0.14	1.19	0.14

References

Bensenouci, F., 2010. Apport des traceurs naturels à la compréhension des transferts au sein des formations argileuses compactées. Thesis, Université Paris-Sud XI, Orsay, France, 194 pp.

Bensenouci, F., Michelot, J.L., Matray, J.M., Savoye, S., Tremosa, J., Gaboreau, S., 2013. Profiles of chloride and stable isotopes in pore-water obtained from a 2000 m-deep borehole through the Mesozoic sedimentary series in the eastern Paris Basin. *Phys. and Chem. of the Earth*, *65*, 1-10.

Blaesi, H.-R., Peters, T. J., Mazurek, M., 1991. Der Opalinus-Ton des Mt. Terri (Kanton Jura): Lithologie, Mineralogie und physiko-chemische Gesteinsparameter. *Nagra Interner Bericht, 90-60.* Nagra, Wettingen, Switzerland.<www.nagra.ch>

Bossart, P., Wermeille, S., 2003. Paleohydrological study of the Mont Terri rock laboratory. In: Heitmann, P., Tripet, J.P. (Eds.), Mont Terri Project-Geology, paleohydrogeoogy and stress field oft he Mont Terri region. Federal Office for Water and Geology Rep. 4, Bern, Switzerland, 45-64. <www.swisstopo.admin.ch>

Bossart, P., Thury, M., 2008. Mont Terri Rock Laboratory. Project, Programme 1996 to 2007 and Results. *Reports of the Swiss Geological Survey, No. 3*, 445 pp. Federal Office of Topography (swisstopo), Wabern, Switzerland. <www.mont-terri.ch>

Bossart, P., Bernier, F., Birkholzer, J., Bruggeman, C., Connolly, P., Dewonck, S., Fukaya, M., Herfort, M., Jensen, M., Matray, J.-M., Mayor, J.C., Moeri, A., Oyama, T., Schuster, K., Shigeta, N., Vietor, T., Wieczorek, K., 2017. Mont Terri rock laboratory, 20 years of research: introduction, site characteristics and overview of experiments. *Swiss J. of Geosci.*, *110*, doi:10.1007/s00015-016-0236-1

Clauer, N., Techer, I., Nussbaum, C., Laurich, B., 2017. Geochemical signatures of paleofluids in microstructures from Main Fault of the Opalinus Clay, Mont Terri rock laboratory, (Switzerland). *Swiss J. of Geosci.*, *110*, doi:10.1007/s00015-016-0253-0

Fierz, T., Rösli, U., 2014. Mont Terri DB Experiment: Installation of a 7-interval multi-packer system into borehole BDB-1. Instrumentation Report. *Mont Terri Technical Note*, TN 20414-23. 37 pp. Federal Office of Topography (swisstopo), Wabern, Switzerland. <www.mont-terri.ch>

Gallagher, K., Charvin, K., Nielsen, S., Sambridge, M., Stephensen, J., 2009. Markov chain Monte Carlo (MCMC) sampling methods to determine optimal models, model resolution and model choice for Earth Science problems. *Mar. and Pet. Geol.*, *26*, 525-535.

Gautschi, A., 2001a. Hydrogeology of a fractured shale (Opalinus Clay): Implications for the deep disposal of radioactive wastes. *Hydrogeol. J.*, *9*, 97-107.

Gonçalvès, J., Violette, S., Wendling, J., 2004. Analytical and numerical solutions for alternative overpressuring processes: applications of the Callovo-Oxfordian argillite in the Paris Basin, France. *J. of Geophy. Res.*, *109(B2)*, DOI: 10.1029/2002JB002278

Gonçalvès, J., Adler, P.M., Cosenza, P., Pazdniakou, A., de Marsily, G., 2015. Semi-permeable membrane properties and chemo-mechanical coupling in clay barriers. *Nat. and Eng. Clay Barriers*, pp. 269-327.

Hostettler, B., Reisdorf, A. G., Jaeggi, D., Deplazes, G., Bläsi, H.-R., Morard, A., Feist-Burkhardt, S., Waltschew, A., Dietze, V., Menkveld-Gfeller, U., 2017. Litho- and biostratigraphy of the Opalinus Clay and bounding formations in the Mont Terri rock laboratory (Switzerland). *Swiss J. of Geosci.*, *110*, doi:10.1007/s00015-016-0250-3

Huysmans, M., Dassargues, A., 2005. Review of the use of Péclet numbers to determine the relative importance of advection and diffusion in low permeability environments. *Hydrogeol. J.*, *13* (5–6), 895–904.

Jacquier, P., Hainos, D., Robinet, J.C., Herbette, M., Grenut, B., Bouchet, A., Ferry, C., 2013. The influence of mineral variability of Callovo-Oxfordian clay rocks on radionuclide transfer properties. *Appl. Clay Sci. 83-84*, 129-136.

Johns, R. T., Vomvoris, S. G., Löw, S., 1995. Review of hydraulic field tests in the Opalinus Clay of Northern Switzerland. *Hydraul. and hydrochem. Charact. of argillaceous rocks.* NEA.

Koroleva, M., Lerouge, C., Mäder, U., Claret, F., Gaucher, E.C., 2011. Biogeochemical processes in a clay formation in situ experiment: Part B - Results from overcoring and evidence of strong buffering by the rock formation. *Appl. Geochem.*, *26 (6)*, 954-966.

Kuhlemann, J., Rahn, M., 2013. Plio-Pleistocene landscape evolution in Northern Switzerland. *Swiss. J. Geosci.*, *106*, 451-467.

Mazurek, M., Elie, M., Hurford, A., Leu, W., Gautschi, A., 2002. Burial history of Opalinus Clay. *Clays In Nat. And Eng. Barriers For Radioact. Waste Confinement*, December 9-12, Reims, France.

Mazurek, M., Hurford, A., Leu, W., 2006. Unravelling the multi-stage burial history of the Swiss Molasse Basin: intergration of apatite fission track, vitrinite reflectance and biomarker isomerisation analysis. *Basin Res., 18*, 27-50.

Mazurek, M., Alt-Epping, P., Bath, A., Gimmi, T., Waber, H.N., Buschaert, S., De Cannière, P., De Craen, M., Gautschi, A., Savoye, S., Vinsot, A., Wemaere, I., Wouters, L., 2011. Natural tracer profiles across argillaceous formations. *Appl. Geochem.*, *26*, 1035-1064

Mazurek, M., de Haller, A., 2017. Pore-water evolution and solute-transport mechanisms in Opalinus Clay at Mont Terri and Mont Russelin (Canton Jura, Switzerland). *Swiss J. of Geosci.*, 110, doi:10.1007/s00015-016-0249-9.

Mills, R.L., and Lobo, V.M.M., 1989. Self-diffusion in Electrolyte Solutions - A Critical Examination of Data Compiled from the Literature. Elsevier.

Novakowski, K.S., Van der Kamp, G., 1996. The radial diffusion method 2. A Semianalytical model for the determination of effective diffusion coefficients, porosity and adsorption. Water Resour. Res., 32, No. 6, 1823-1830.

Noy, D., Horseman, S., Harrington, J., Bossart, P., Fisch, H., 2004. An Experimental and modelling study of chemico-osmotic effects in the Opalinus Clay of Switzerland. In: Heitzmann, P. ed. (2004) Mont Terri Project - Hydrogeological Synthesis, Osmotic Flow. *Rep. of the Fed. Off. for Water and Geol.* (FOWG), Geology Series (6), 95–126.

Nussbaum, C., Bossart, P., Amann, F., Aubourg, C., 2011. Analysis of tectonic structures and excavation induced fractures in the Opalinus Clay, Mont Terri underground rock laboratory (Switzerland). *Swiss J. of Geosci., 104*, 187-210.

Nussbaum, C., Kloppenburg, A., Caer, T., Bossart, P., 2017. Tectonic evolution of the Mont Terri anticline based on forward modelling. *Swiss J. of Geosci.*, 110, doi:10.1007/s00015-016-0248-x

Patriarche, D., Michelot, J.L., Ledoux, E., Savoye, S., 2004a. Diffusion as the main process for mass transport in very low water content argillites: 1. Chloride as a natural tracer for mass transport – Diffusion coefficient and concentration measurements in interstitial water. *Water Resour. Res.*, 40, W01516, doi:10.1029/2003WR002700.

Patriarche, D., Michelot, J.L., Ledoux, E., Savoye, S., 2004b. Diffusion as the main process for mass transport in very low water content argillites: 2. Fluid flow and mass transport modeling. *Water Resour. Res.*, 40, W01517, doi:10.1029/2003WR002700.

Pearson, F. J., Arcos, D., Boisson, J-Y., Fernández, A. M., Gäbler, H.E., Gaucher, E., Gautschi, A., Griffault, L., Hernán, P., Waber, N., 2003. Mont Terri Project - Geochemistry of water in the Opalinus Clay Formation at the Mont Terri Rock Laboratory. *Rep. of the Swiss Geol. Survey, No. 5*, 143 pp. Federal Office of Topography (swisstopo), Wabern, Switzerland. <www.mont-terri.ch>

Petersen, J.O, Deschamps, P., Gonçalvès, J., Hamelin, B., Michelot, J.L., Guendouz, A., Zouari, K., 2014. Quantifying paleorecharge in the Continental Intercalaire (CI) aquifer by a Monte-Carlo inversion approach of $^{36}Cl/Cl$ data. *Appl.Geochem*, *50*, 209-221

Sacchi, E., Michelot J-L., Pitsch, H., Lalieux, P., Aranyossy, J-F., 2001. Extraction of water and solutes from argillaceous rocks for geochemical characterisation: Methods, processes, and current understanding, *Hydrogeol. J.*, *9*, 17-33.

Sellin, P., Leupin, O.X., 2014. The use of clay as an engineered barrier in radioactive waste management – a review. *Clays and Clay Miner.*, *61*, 477–498.

Soler, J.M., 2001. The effect of coupled transport phenomena in the Opalinus Clay and implications for radionuclide transport. *J. of Contam. Hydrol.*, 53, 63–84

Tarantola, A., 2005. Monte Carlo Methods. Chapter 2 in Inverse Problem Theory and Methods for Model Parameter Estimation. *Soc. for Ind. and Appl. Math.*, 41-56.

Van der Kamp, G., Van Stempvoort, D.R., Wassenaar, L.I., 1996. The radial diffusion method 1. Using intact cores to determine isotopic composition, chemistry, and effective porosities for groundwater in aquitards. *Water Resour. Res.*, *32*, *No. 6*, 1815-1822.

Van der Lee, J., De Windt, L., Lagneau V., Goblet, P., 2003. Module-oriented modeling of reactive transport with HYTEC. *Comput. & Geosci.*, *29-3*, 265-275.

Van Loon, L.R., Soler, J., Müller, W. and Bradbury, M. H., 2004. Anisotropic diffusion in layered Argillaceous Rocks: a case study with Opalinus clay. *Environ. Sci. Technol.*, *38*, 5721–5728.

Wersin, P., Waber, H.N., Mazurek, M., Mäder, U.K., Gimmi, T., Rufer, D., Traber, D., 2013. Resolving Cl and SO_4 profiles in a clay-rich rock sequence. *Procedia Earth and Planet. Sci*,. 7, 892-895.

Yu, C., Matray, J.M., Gonçalvès, J., Jaeggi, D., Gräsle, W., Wieczorek, K., Vogt, T., Sykes, E., 2017. Comparative study of methods to estimate hydraulic parameters in the hydraulically undisturbed Opalinus Clay (Switzerland). *Swiss J. of Geosci.*, *110*, doi: 10.1007/s00015-016-0257-9h)